Heliyon 11 (2025) e41505

Contents lists available at ScienceDirect

Heliyon

journal homepage: www.cell.com/heliyon

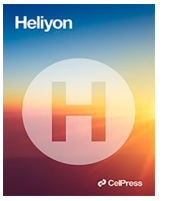

Research article

Comparative analysis of petal phytoconstituents reveals insights into the characteristics of an under-reported edible old rose variety native to Chongqing, China

Chan Xu [a,b,*], Yuan Chen [a], Zongli Hu [b], Qiaoli Xie [b], Hang Guo [a], Shibing Tian [a,**], Guoping Chen [b,***]

[a] Institute of Vegetables and Flowers, Chongqing Academy of Agricultural Sciences, Chongqing, 400000, China
[b] College of Bioengineering, Chongqing University, Chongqing, 400000, China

ARTICLE INFO

Keywords:
Edible flower
Old rose
Phytoconstituents
Floral scent
Floral color
Metabolic pathway

ABSTRACT

Chongqing Old Rose is an ancient edible rose variety native to Chongqing, China, but is under-reported. Further evidence is required to fully establish its potential benefits. The complete metabolic profiles were examined for comparative analysis between the Old Rose and three rose cultivars. The results showed that the pathways of flavonoid biosynthesis, monoterpenoid biosynthesis, and phenylalanine metabolism were significantly enriched in Old Rose. The predominant anthocyanins in Old Rose were cyanidin and peonidin, which may contribute to flower coloration and indicate the antioxidant potential of this plant. Additionally, this plant was rich in aromatic compounds and terpenoids such as 2-phenylethanol, linalool, geraniol, and caryophyllene α-oxide, indicating that it has a natural basis for extracting essential oil. Moreover, the presence of some active phytoconstituents, such as phenols, steroids, and alkaloids, also suggests its potential for edible and medicinal applications besides flavonoids and terpenoids.

1. Introduction

Rose is a common name for the genus *Rosa*, which belongs to the Rosaceae family and contains approximately 200 species. Although it is an economically important crop in ornamental horticulture, some roses are used in pharmaceuticals, flavors, and fragrances. Its use for vomiting blood, stomachache, acute mastitis, and other diseases was recorded in the Supplement of Materia Medica (Bencao Shiyi, the 8th century CE (CE: Common Era)). A food recipe for the rose was recorded and attributed to Apicius as early as the first century Common Era [1]. Moreover, rose extracts of petals have been used in the perfume and cosmetic industries [2].

In China, "Meigui" is an umbrella word for some rose varieties that are usually cultivated for extracting rose essential oil, making rose tea, rose wine, rose sauce, and pharmaceuticals [3,4]. It is also known internationally as the traditional rose, namely, Old Rose. Unlike many rose cultivars grown to produce cut flowers or for ornamental purposes, which are often brightly colored but lack aroma, Meigui is usually fragrant and edible. Following the investigations conducted in recent years, approximately 20 edible cultivars have been used in China [3,5]. However, these investigations did not fully reveal edible rose varieties in China. The Chongqing Old Rose, as

* Corresponding author. Institute of Vegetables and Flowers, Chongqing Academy of Agricultural Sciences, Chongqing, 400000, China.
** Corresponding author.
*** Corresponding author.
E-mail address: xchan8808@163.com (C. Xu).

https://doi.org/10.1016/j.heliyon.2024.e41505
Received 30 August 2024; Received in revised form 6 November 2024; Accepted 25 December 2024
Available online 26 December 2024

a local variety, can also be included in Meigui and is utilized in food processing. It has a long and storied history, but it has not been mentioned in previous academic literature. With petals as the essential ingredients for aroma and flavor, Chongqing Province in southwestern China is well known for its rose flower crunchy rice candy ("Meiguipai Mihuatang" in Chinese; Qing Dynasty).

Recently, as flowers have become increasingly popular as edible fresh crops worldwide [6], the edible value of roses has been widely noticed [4,7]. As a food resource, rose petals are natural products with a nutritive value that can offer several phytoconstituents, including pigments, flavonoids, anthocyanins, sugars, organic acids, and dietary fiber [4,8]. Studies on the chemical composition and properties of edible rose petals are linked to the presence of several biologically active phytoconstituents, together with an increased awareness of consumers regarding the consumption of natural sources of active phytoconstituents [9–13].

The phytoconstituents of rose petals are liable for their pharmacological activity besides nutritional value. In recent years, pharmacological studies have been conducted on human healthcare, and they have proven many benefits. They have been used for eye diseases [14], antidiabetic activity [15,16], and antianxiety, anti-inflammatory, antioxidant, and anticholinesterase activities [17]. Moreover, phytoconstituent-based alternative medicines are cheaper, easily accessible, and have fewer side effects with better tolerance [18,19].

Aside from consumption value, phytoconstituents are responsible for the color, aroma, and other physiological properties of plants. The anthocyanins among the phytoconstituents determine the flower coloration. The volatile organic compounds among the phytoconstituents determine aroma characteristics as a mixture of volatile substances with low molecular weight and high vapor pressure at ambient temperatures. The physical properties of these compounds allow them to freely cross cellular membranes and be emitted into the surrounding environment [20]. The volatile organic compounds in rose petals mainly include terpenoids, phenylpropanoids/benzenoids, fatty acid derivatives, and amino acid derivatives, in addition to a few species-/genus-specific compounds not represented in those major classes [21]. Volatile organic compounds are an adaptive mechanism by which plants attract pollinators and resist pests and diseases [22,23].

In this study, we aimed to investigate the phytoconstituents of the Chongqing Old Rose to understand the coloration and floral fragrance formation and assess its medicinal and edible potential. We performed comparative analyses on the Chongqing Old Rose alongside three reference cultivars, each distinguished by varying colors and floral fragrances. Petal phytoconstituents were analyzed using comprehensive non-targeted metabolomics analysis. We constructed reaction networks of key metabolites to depict their biosynthesis and expand our understanding of coloration and floral fragrance formation mechanisms. The results can provide valuable knowledge on the potential value of perfume, natural flavor, medicine, and functional food. They can contribute to increasing the commercial value and producing a healthier product for consumers.

2. Materials and methods

2.1. Plant materials

The Chongqing Old Rose was used as the target plant, this plant is abbreviated as Old Rose in the text. This plant has red flowers with a strong fragrance (Fig. 1A). Three other varieties, including *Rosa* x hybrid cv. 'Damascena', *Rosa* x hybrid cv. 'Crimson Glory', and *Rosa* x hybrid cv. 'Iceberg', were used for comparative analysis. The four roses were introduced from a commercial production nursery, the Jianlong Rose Garden (Chongqing, China, 106°2′E, 29°4′N), and grown in the nursery of the Chongqing Academy of

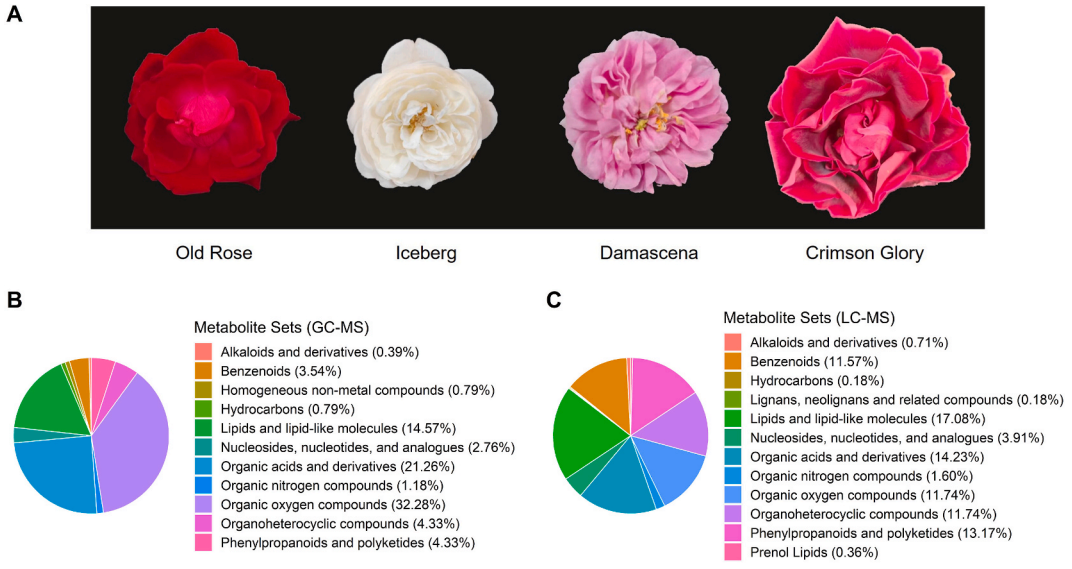

Fig. 1. Flowers of the four roses and the category of the detected phytoconstituents.

Agricultural Sciences. Iceberg has white, almost scentless flowers, which bloom in large numbers for a long time and are most often used to decorate parks and streets (Fig. 1A). Damascena has pink flowers with a strong fragrance, is an edible cultivar, and is often commercially cultivated as an oil-bearing rose (Fig. 1A). Crimson Glory has deep red flowers with a strong fragrance and is also an edible cultivar, often grown commercially as a tea rose (Fig. 1A). Petals of the four plants from fully unfolded flowers used for the experiment were collected around 9 a.m. All petal samples were frozen in liquid nitrogen and stored at a −80 °C refrigerator.

2.2. Gas chromatography-time-of-flight mass spectrometry (GC-TOF/MS)

Non-targeted metabolomic analysis was performed on GC-TOF/MS at PANOMIX company. The GC-TOF/MS is abbreviated as GC-MS in the text. The protocol for GC-MS metabolite extraction followed that of a previous study [24]. Briefly, 60 mg of the sample was placed in a 2 mL Eppendorf (EP) tube. Moreover, 0.5 mL of a mixed solution (acetonitrile:isopropanol:water = 3:3:2, v/v/v) (−20 °C) and four zirconium beads (diameter 2 mm) were added. The tube was placed in a high-flux tissue grinder, shocked at 30 Hz for 20 s, held still for 10 s, cycled eight times, and sonicated for 5 min in an ice water bath. Then 0.5 mL of the mixed solution (acetonitrile: isopropanol:water = 3:3:2, v/v/v) was added to the tube and sonicated for 5 min in an ice water bath. The tube was then centrifuged at 12,000 rpm for 2 min, and 500 μL of the supernatant solution was transferred to a new 2 mL EP tube. The supernatant was concentrated to dryness (8–10 h) using a vacuum concentrator. Next, 80 μL of 20 mg/mL MEOX solution was added for re-dissolution, vortexed for 30 s, and incubated at 60 °C for 60 min. Then, 100 μL of BSTFA-TMCS (99:1) reagent was added, incubated at 70 °C for 90 min, and centrifuged at 14,000 rpm for 3 min to obtain the supernatant. Next, 90–100 μL of the supernatant was placed in a detection bottle for GC-TOF/MS detection. The used chemicals are displayed in Supplementary Table S1.

To separate the derivatives, a DB-5MS capillary column (30 m × 0.25 mm i.d., 0.25 μm film thickness, Agilent J & W Scientific, Folsom, CA, USA) was used with a constant flow of 1 mL/min helium. The auto-sampler injected 1 μL of the sample in the split mode with a split ratio of 1:10. The injection temperature was 280 °C. The temperatures of the transfer line ion source were 320 and 230 °C, respectively. The temperature rise programs were followed by an initial temperature of 50 °C for 0.5 min, 15 °C/min up to 320 °C, and maintained at 320 °C for 9 min. The full scan method was used for mass spectrometry, with a scan rate of 10 spec/s, electron energy of −70 V, and solvent delay of 3 min [25].

2.3. Ultra-high-performance liquid chromatography/electrospray ionization-mass spectrometry (MS) analysis (UHPLC–ESI–MS/MS)

Non-target metabolomic analysis was employed for UHPLC–ESI–MS/MS which is abbreviated as LC-MS in the text. These analyses were also performed using PANOMIX. Briefly, the sample was weighed and placed into a 2 mL centrifuge tube, and 600 μL MeOH containing 4 ppm 2-amino-3-(2-chloro-phenyl)-propionic acid (stored at −20 °C) was added and vortexed for 30 s. Then, 100 mg of glass beads were added and placed in a tissue grinder for 90 s at 60 Hz. Room-temperature ultrasound was conducted for 15 min, followed by centrifugation for 10 min at 12,000 rpm and 4 °C. The supernatant was filtered by 0.22 μm membrane and transferred into a detection bottle for LC-MS detection [26].

A Vanquish UHPLC System (Thermo Fisher Scientific, USA) and an ACQUITY UPLC ® HSS T3 (150 × 2.1 mm, 1.8 μm) column (Waters, Milford, MA, USA) were employed for LC analysis. The column temperature, flow rate, and injection volume were set to 40 °C, 0.25 mL/min, and 2 μL, respectively. For LC-ESI (+)-MS analysis, the mobile phase consisted of (C) 0.1 % formic acid in acetonitrile (v/v) and (D) 0.1 % formic acid in water (v/v). Separations were performed under the following gradient: 0–1 min, 2 % C; 1–9 min, 2 %–50 % C; 9–12 min, 50 %–98 % C; 12~13.5 min, 98 % C; 13.5–14 min, 98 %–2 % C; 14–20 min, 2 % C. For LC-ESI (−)-MS analysis, the analytes were analyzed using (A) acetonitrile and (B) ammonium formate (5 mM). Separations were conducted under the following gradient: 0–1 min, 2 % A; 1–9 min, 2 %–50 % A; 9–12 min, 50 %–98 % A; 12~13.5 min, 98 % A; 13.5–14 min, 98 %–2 % A; 14–17 min, 2 % A [27]. The used chemicals are displayed in Supplementary Table S1.

We performed mass spectrometric detection of the metabolites using a Thermo Q Exactive (Thermo Fisher Scientific, USA) detector with an ESI ion source. Simultaneous MS1 and MS/MS (Full MS-ddMS2 mode and data-dependent MS/MS) acquisitions were used. The parameters were as follows: Sheath gas pressure, 30 arb; Aux gas flow, 10 arb; spray voltage, 3.50 kV ESI(+) and −2.50 kV ESI(−); capillary temperature, 325 °C; MS1 range, *m/z* 81–1000; MS1 resolving power, 70000 FWHM; number of data-dependent scans per cycle, 10; MS/MS resolving power, 17500 FWHM; normalized collision energy, 30 %; dynamic exclusion time, automatic [28].

2.4. Metabolite profiles analysis

All detected phytoconstituents were annotated with the HMDB, Massbank, LipidMaps, Mzcloud, Kyoto Encyclopedia of Genes and Genomes (KEGG), and PANOMIX databases to obtain the metabolite profiles of all samples.

MetaboAnalyst software (version 6.0) (http://www.metaboanalyst.ca) was used to analyze the metabolic pathways. The metabolic pathway analysis module combines results from powerful pathway enrichment analysis with pathway topology analysis to help researchers identify the most relevant pathways involved in the conditions under study. To identify the target pathways, the impact value threshold calculated from pathway topology analysis was set to 0.1. We constructed reaction networks of the target pathways based on the KEGG map to depict the biosynthesis of the key metabolites.

2.5. Statistical

Different multivariate statistical methods were applied to extract the most useful information. We used principal component

analysis (PCA) and partial least squares discriminant analysis (PLS-DA) to determine intrinsic clusters within the dataset and to obtain separation. We applied orthogonal partial least squares discriminant analysis (OPLS-DA) to produce models to discern group differences and similarities. PCA, PLS-DA, and OPLS-DA were performed using the "ropls" function in R software (version 4.3.1). The relative importance of each metabolite in the OPLS-DA model was evaluated using variable importance in projection (VIP) values. Metabolites with VIP $\geq$1 and |log2fold change| $\geq$ 1 were considered differentially accumulated metabolites (DAMs).

3. Results

3.1. Phenotype of the plant materials

Three roses with different uses were selected for a comparative analysis to reveal the characteristics of the Chongqing Old Rose. Iceberg, Crimson Glory, and Damascena serve as cut flowers, flower tea, and oil-bearing cultivars, respectively. The flowers of the four roses differed in color, scent, and size. First, the Iceberg's flower has almost no color (white), while the other three are colored in different shades of red. These visual color differences were supposed to be related to anthocyanins, as the deeper the color, the higher the levels of anthocyanins. Therefore, the metabolic activities of the supposed pigments were as follows: Crimson Glory > Chongqing Old Rose > Damascena > Iceberg. Second, the Iceberg has no or mild scent, while the other three have strong floral fragrances. Petals with or without fragrance may be related to the inhibition or activation of floral scent metabolic pathways. Additionally, the flowers of Crimson Glory were larger than those of Chongqing Old Rose, Damascena, and Iceberg (Fig. 1A). Due to these differences, samples can also be divided into four groups by color and two groups by scent. Furthermore, floral phenotypic features may be related to the type and level of phytoconstituents.

3.2. Overview of GC-MS and LC-MS data

To identify the characteristics of Old Rose, the phytoconstituents were subjected to GC-MS and LC-MS. Typical total ion chromatograms (TICs) are presented in Figs. S1–2. A total of 254 phytoconstituents were identified by GC-MS, and they were categorized within 11 super classes in the MetaboAnalyst (version 6.0) system, including 82 organic oxygen compounds, 54 organic acids and derivatives, 37 lipids and lipid-like molecules, 11 phenylpropanoids and polyketides, 11 organoheterocyclic compounds, 9 benzenoids, 7 nucleosides/nucleotides and analogues, 3 organic nitrogen compounds, 2 homogeneous non-metal compounds, 2 hydrocarbons, and 1 alkaloids and derivatives, and 35 additional compounds that did not fit into this system (Fig. 1B). A total of 561 phytoconstituents were identified by LC-MS, and they were categorized into 12 super classes, including 96 lipids and lipid-like

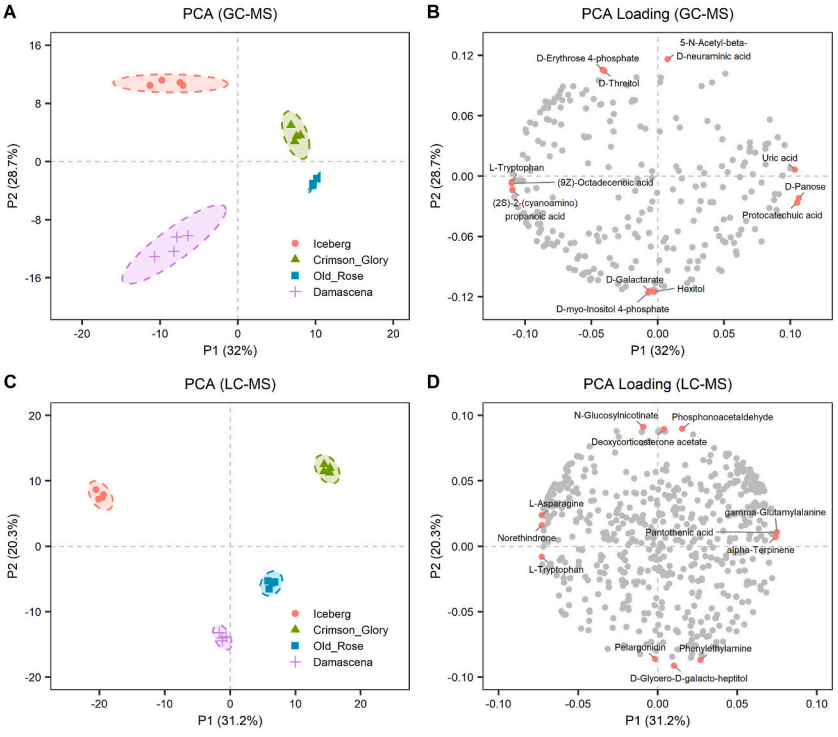

Fig. 2. PCA analysis for petals of the four rose varieties. (A) PCA score plot of GC-MS data. (B) Loading plot of GC-MS data. (C) PCA score plot of LC-MS data. (D) Loading plot of LC-MS data.

molecules, 80 organic acids and derivatives, 74 phenylpropanoids and polyketides, 66 organic oxygen compounds, 66 organo-heterocyclic compounds, 65 benzenoids, 22 nucleosides/nucleotides and analogues, 9 organic nitrogen compounds, 4 alkaloids and derivatives, 2 prenol lipids, 1 lignan/neolignans and related compounds, 1 hydrocarbon, and 75 additional compounds that did not fit into this system (Fig. 1C). These metabolites may represent major metabolic activities in the petals. All compounds were subdivided into further subgroups, and Supplementary Fig. S3 displays the top 25 groups. The results illustrated that rose petals were rich in bioactive phytoconstituents, including flavonoids, phenols, cinnamic acids, steroids, and tannins (Fig. S3).

3.3. Accumulation patterns of metabolites

Differences in the accumulation patterns of metabolites in these cultivars were analyzed using PCA, PLS-DA, and clustering heatmaps. The results of PCA analysis indicated that there were notable separations in different cultivars in both GC-MS and LC-MS data. First, PCA analysis of the GC-MS dataset revealed that the Old Rose and Crimson Glory were separated from Iceberg and Damascena on PC1 with 32 % variance. In comparison, the Old Rose and Damascena were separated from Iceberg and Crimson Glory on PC2 with 28.7 % variance (Fig. 2A). Furthermore, the PCA loading plot of the GC-MS dataset depicted the compounds that contributed to separation. Along with PC1, D-panose, protocatechuic acid, and uric acid were observed as major contributors to the discrimination between Old Rose and Crimson Glory. Along PC2, high levels of D-threitol and D-erythrose 4-phosphate were detected in Iceberg. However, D-myo-inositol 4-phosphate, hexitol, and D-galactarate were abundant in Damascena (Fig. 2B). Contrarily, the PCA analysis of LC-MS dataset revealed that the four cultivars were separated from each other on the PC1 axis and explained 31.2 % variance, while Iceberg and Crimson Glory were separated from Old Rose and Damascena on PC2 and explained 20.3 % variance (Fig. 2C). Along PC1, pantothenic acid, α-terpinene, and gamma-glutamylalanine were increased in Damascena, Old Rose, and Grimson Glory, whereas L-asparagine, L-tryptophan, and norethindrone were abundant in Iceberg. Along PC2, N-glucosylnicotinate, deoxycorticosterone acetate, and phosphonoacetaldehyde were observed as major contributors to the discrimination of Iceberg and Crimson Glory. At the same time, phenylethylamine, pelargonidin, and D-glycero-D-galacto-heptitol were abundant in Old Rose and

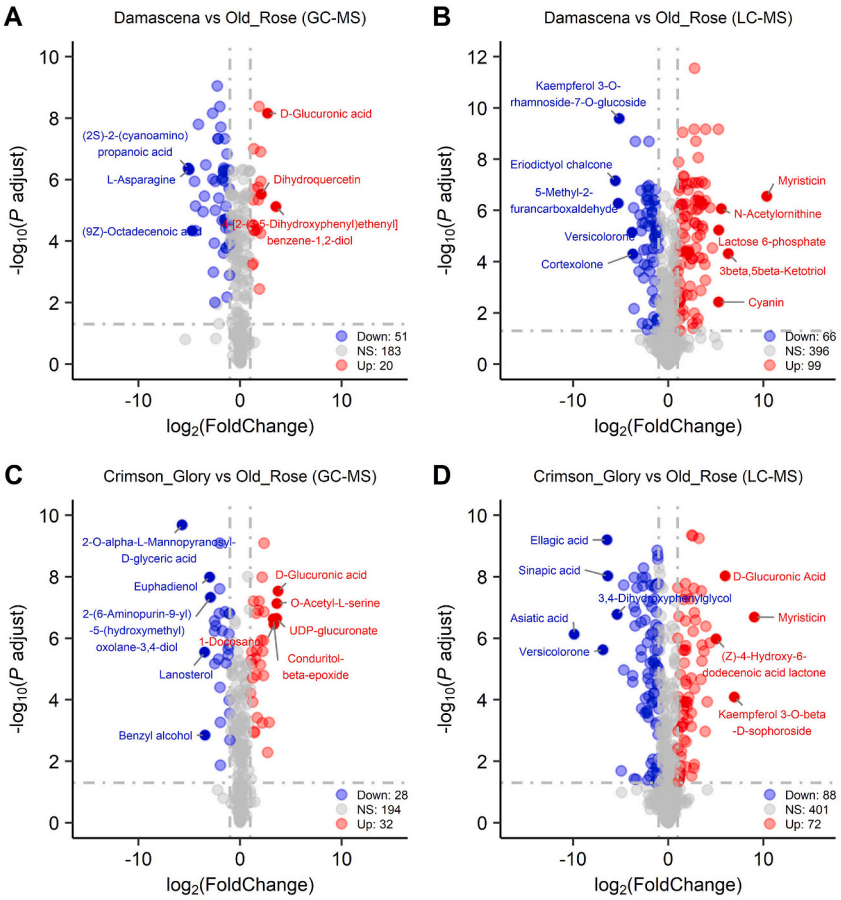

Fig. 3. Differential metabolites selection between fragrant roses by volcano plots. (A) Volcano plot of differential metabolite in Damascena vs Old Rose based on GC-MS data. (B) Volcano plot of differential metabolites in Crimson Glory vs Old Rose based on GC-MS data. (C) Volcano plot of differential metabolites in Damascena vs Old Rose based on LC-MS data. (D) Volcano plot of differential metabolites in Crimson Glory vs Old Rose based on LC-MS data.

Damascena (Fig. 2D). Next, the results of PLS-DA were similar to those of PCA. Additionally, each model exhibited a high degree of goodness of fit and predictive capability, as confirmed by a 200 times random permutation test. Specifically, the R^2Y and Q^2 values for the GC-MS data were 0.998 and 0.966, respectively, and for the LC-MS data, the R^2Y and Q^2 values were 0.998 and 0.963, respectively (Fig. S4).

The results of the cluster heatmap analysis depicted that there were significant differences in metabolites in different cultivars, which were divided into four clusters. The GC-MS metabolites in cluster 1 were the highest in Crimson Glory, in cluster 2 were the highest in Old Rose, in cluster 3 were the highest in Damascena, and in cluster 4 were the highest in Iceberg (Fig. S5). The LC-MS metabolites in cluster 1 were abundant in Iceberg, cluster 2 was abundant in Crimson Glory, cluster 3 was abundant in Old Rose, and cluster 4 was abundant in Damascena (Fig. S5). The different replicates were similarly clustered, indicating good homogeneity between replicates and high reliability of the data.

3.4. Comparison of metabolite profiles among four roses

To further depict the similarities and differences between Old Rose and the other three rose cultivars, OPLS-DA was performed to analyze the metabolite profiles of petals. Variables with VIP >1 and *P*-adjust <0.05 were considered differentially accumulated metabolites (DAMs). A DAM was considered downregulated if $\log_2$(fold change) < -1 or upregulated if $\log_2$(fold change) > 1.

Old Rose is a fragrant phenotype similar to Damascena and Crimson Glory, whereas Iceberg is a scentless phenotype. Therefore, a comparison among the fragrant roses could help to make the characteristics of Old Rose explicit. A comparison between fragrant cultivars and scentless roses could explain aroma formation. Metabolomics similarity was revealed by an overview of the ratios of metabolites with non-significant difference in expression, and 71.04 %, 73.01 %, 58.40 %, 61.72 %, and 58.77 % of non-significant metabolites were identified between Damascena versus Old Rose, Crimson Glory versus Old Rose, Iceberg versus Old Rose, Iceberg versus Damascena, Iceberg versus Crimson Glory, respectively. These results indicated that the similarities in metabolic profiles between fragrant roses were higher than those between fragrant and scentless roses.

The volcano plots of two comparison groups of fragrant roses are displayed in Fig. 3. Metabolite names with the largest fold change values were displayed in the volcano plot. Compared with Damascena, the Old Rose significantly accumulated 119 DAMs (GC-MS: 20 DAMs, LC-MS: 99 DAMs), of which the metabolite with the largest fold change was myristicin, followed by 3beta,5beta-ketotriol, N-acetylornithine, lactose 6-phosphate, cyanin, and dihydroquercetin (Fig. 3A–B). Compared with Crimson Glory, the Old Rose

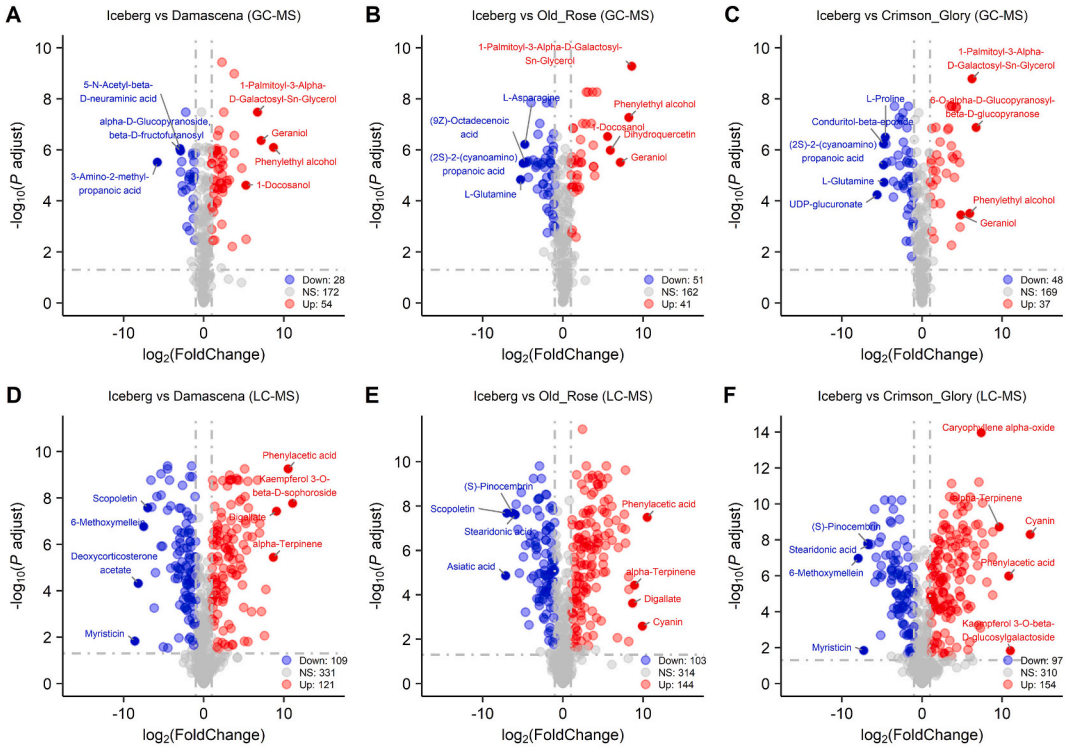

Fig. 4. Differential metabolites selection between fragrant and scentless roses by volcano plots. (A) Volcano plot of differential metabolites in Iceberg vs Damascena based on GC-MS data. (B) Volcano plot of differential metabolites in Iceberg vs Old Rose based on GC-MS data. (C) Volcano plot of differential metabolites in Iceberg vs Crimson Glory based on GC-MS data. (D) Volcano plot of differential metabolites in Iceberg vs Damascena based on LC-MS data. (E) Volcano plot of differential metabolites in Iceberg vs Old Rose based on LC-MS data. (F) Volcano plot of differential metabolites in Iceberg vs Crimson Glory based on LC-MS data.

significantly accumulated 104 DAMs (GC-MS: 32 DAMs, LC-MS: 72 DAMs), of which the metabolite with the largest fold change was myristicin, followed by Kaempferol 3-O-beta-D-sophoroside, and then D-glucuronic acid, and (Z)-4-hydroxy-6-dodecenoic acid lactone (Fig. 3C–D). Compared with Old Rose, 117 DAMs (GC-MS: 51 DAMs, LC-MS: 66 DAMs) were accumulated in Damascena, which largely accumulated some amino acids, flavonoids, and fatty acids, such as L-asparagine, (9Z)-octadecenoic acid, L-tryptophan, (2S)-2-(cyanoamino)propanoic acid, and kaempferol 3-O-rhamnoside-7-O-glucoside (Fig. 3A–B). Moreover, 116 DAMs (GC-MS: 28 DAMs, LC-MS: 88 DAMs) were accumulated in Crimson Glory, of which versicolorone, ellagic acid, sinapic acid, asiatic acid, 2-O-α-L-mannopyranosyl-D-glyceric acid, and sphingosine were largely accumulated (Fig. 3C–D).

The volcano plots of three comparison groups between fragrant and scentless roses are displayed in Fig. 4. Compared with Iceberg, there were 54, 41, and 37 upregulated metabolites based on GC-MS data in Damascena, Old Rose, and Crimson Glory, respectively, and the corresponding numbers of downregulated metabolites were 28, 51, and 48, respectively (Fig. 4A–C). Notably, some of the specific fragrant metabolites, such as geraniol, phenylethyl alcohol, and α-terpinene, significantly accumulated in the aromatic roses, while some amino acids and carbohydrates, including asparagine, phenylalanine, glutamine, and proline, accumulated in the Iceberg. For the LC-MS dataset, there were 121, 144, and 154 upregulated metabolites in Damascena, Old Rose, and Crimson Glory, respectively, and the corresponding numbers of downregulated metabolites were 109, 103, and 97, respectively (Fig. 4D–F). Next, we generated a DAM dataset by taking the intersection of upregulated metabolites using Venn analysis. The GC-MS dataset yielded 23 overlapping metabolites, while the LC-MS dataset yielded 71 (Fig. S6). After removing duplicates, 93 key metabolites were obtained by merging the overlapping metabolites from GC-MS and LC-MS, and the metabolites with fold change values over 10 in all three comparison groups are displayed in Supplementary Table S2. Some pigments, flavonoids, and aromatic compounds, such as α-terpinene, phenylacetic acid, cyanin, cyanidin 3-O-rutinoside, and delphinidin 3-rutinoside, accumulated significantly in fragrant roses (Table S2), which could potentially be linked to floral fragrance formation and coloration.

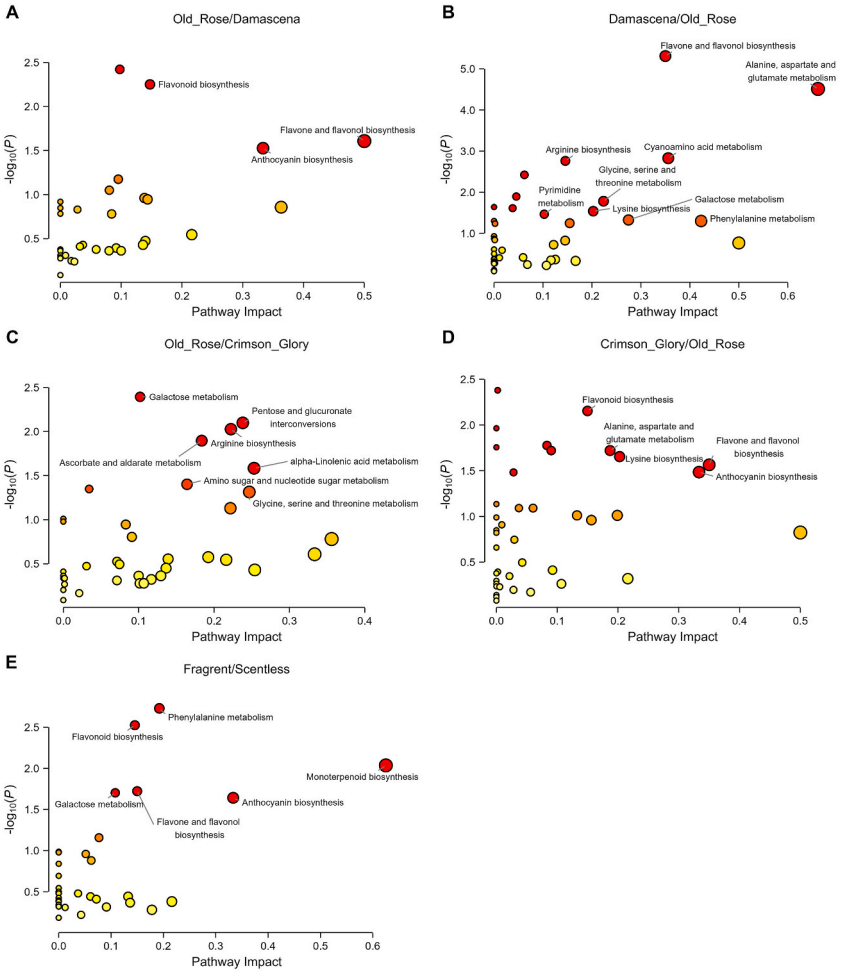

Fig. 5. Metabolic pathway analysis of the selected differential metabolites. (A) Main metabolic pathways of Old Rose in Old Rose vs Damascena. (B) Main metabolic pathways of Damascena in Old Rose vs Damascena. (C) Main metabolic pathways of Old Rose in Old Rose vs Crimson Glory. (D) Main metabolic pathways of Crimson Glory in Old Rose vs Crimson Glory. (E) Main metabolic pathways of the selected differential metabolites between fragrant and scentless roses.

3.5. Metabolic pathway analysis

Based on the identified DAMs, the metabolic pathways involved in the differences among rose cultivars were analyzed. In Damascena versus Old Rose, the results suggested that the metabolites that specifically accumulated in Old Rose were mainly enriched (raw $P < 0.05$ and impact value > 0.1) in flavonoid biosynthesis, flavone and flavonol biosynthesis, and anthocyanin biosynthesis (Fig. 5A). However, in Damascena, there were nine significant pathways, including secondary metabolite (flavone and flavonol biosynthesis) and some amino acids, nucleotide, and carbohydrate metabolism pathways (Fig. 5B). In Crimson Glory vs Old Rose, there were 7 potential target pathways identified in Old Rose including some amino acid, lipid, and carbohydrate metabolism (Fig. 5C). While there were 5 potential target pathways identified in Crimson Glory including amino acid, lipid, and secondary metabolites metabolism pathways (Fig. 5D). The primary difference in the comparison between Old Rose and Damascena or Crimson Glory was the biosynthesis of flavonoids, suggesting that the most dominant difference in their biosynthetic process was flower coloration. In contrast, to further clarify the relationships between fragrant and scentless roses, the dataset with overlapping metabolites (93 DAMs) accumulated in fragrant cultivars was analyzed. Six potential target pathways were identified, including phenylalanine metabolism, flavonoid biosynthesis, monoterpenoid biosynthesis, flavone and flavonol biosynthesis, galactose metabolism, and anthocyanin biosynthesis (Fig. 5E). In summary, phenylalanine metabolism, monoterpenoid biosynthesis, and biosynthesis of flavonoids stood out in the comparison groups; the first two pathways were involved in aroma formation, and the biosynthesis of flavonoids was involved in the coloration of flowers.

Furthermore, the compounds related to the five outstanding pathways were mapped to KEGG pathways to depict their biosynthetic reactions in rose petals. Figs. 6 and 7 illustrate the monoterpenoid biosynthesis and phenylalanine metabolism pathways, respectively, and list the pathway-related compounds as heatmaps. Pathways of flavonoid biosynthesis are displayed in Supplementary Figs. S7–9. Construction of the compound reaction network helps us understand the biosynthesis of target metabolites. Phenylethyl alcohol, an essential rose aroma compound, was significant in fragrant roses; however, its precursor phenylacetaldehyde was absent in our metabolite profiles. This suggests that there may be an unclear reaction pathway for biosynthesis.

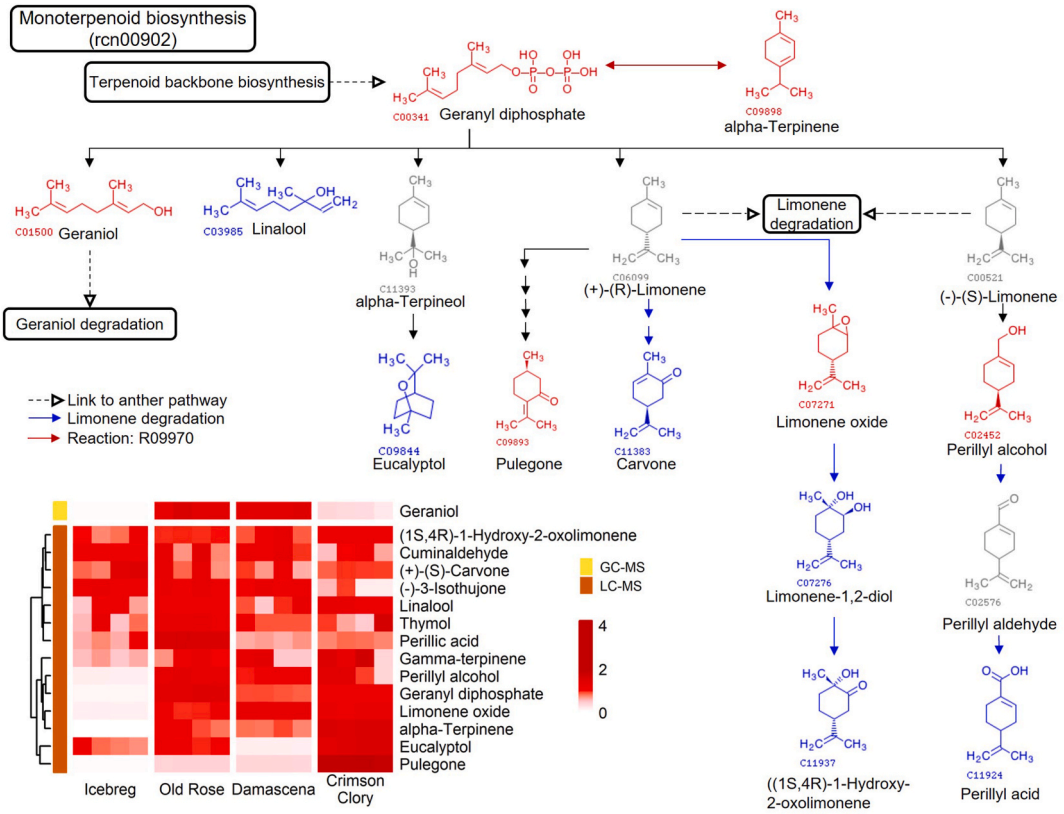

Fig. 6. Diagram of monoterpenoid biosynthesis and pathway-related compounds. The identified monoterpenoids were mapped to KEGG pathway rcn00902, and the heatmap shows scaled values for relative concentrations. Compounds marked in red: significantly presented in three fragrant roses. Compounds marked in blue: presented in metabolite profiles. Compounds marked in gray: not detected.

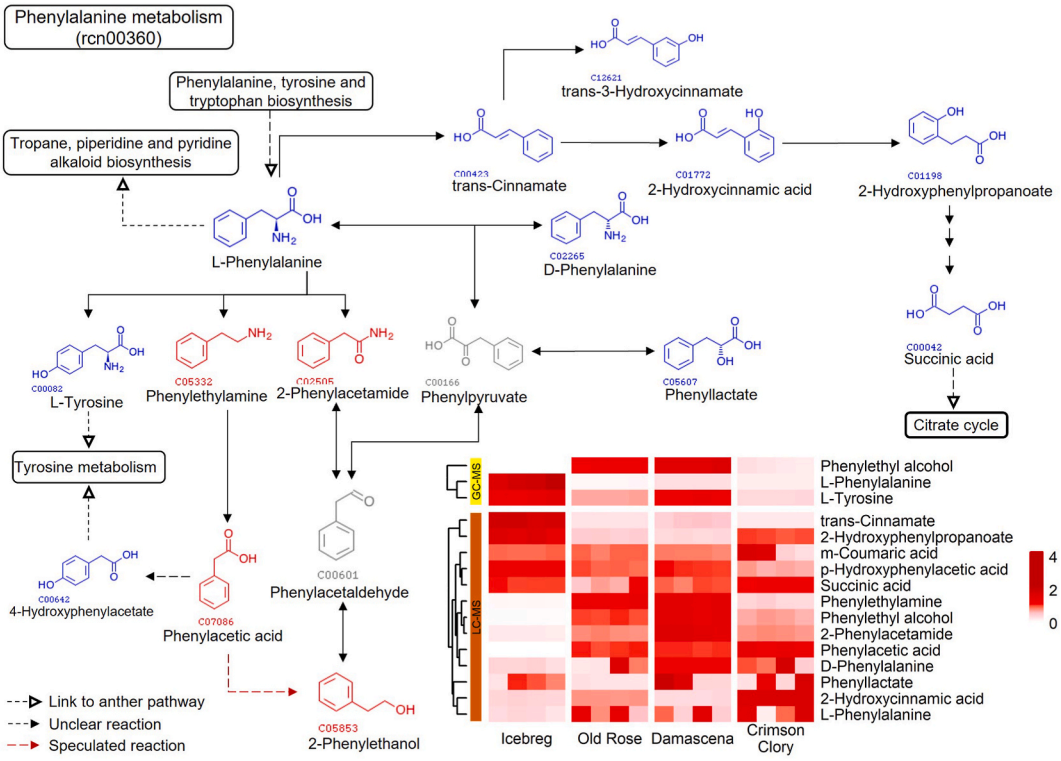

Fig. 7. Diagram of phenylalanine metabolism and pathway-related compounds. The identified pathway-related compounds were mapped to KEGG pathway rcn00360, and the heatmap shows scaled values for relative concentrations. Compounds marked in red: significantly presented in three fragrant roses. Compounds marked in blue: presented in metabolite profiles. Compounds marked in gray: not detected.

4. Discussion

Petals are staple products of roses and are widely used for food, oil extraction, and as raw materials in the pharmaceutical processing industry. LC-MS and GC-MS are efficient methods for screening and identifying phytoconstituents in plants [29–31]. Consequently, these two methods were employed to detect the phytoconstituents in the petals. Phytoconstituents are responsible for the color, flavor, and aroma and for their pharmacological activity, which determines their potential development value. Organoleptic quality may serve as a basis for speculating on plant phytoconstituents and predicting their value. Here, the Old Rose flowers are bright red, and a strong fragrant may predict the enrichment of the pigment and floral aroma compounds.

The colors of plant petals are caused by anthocyanins and phenolic compounds from the flavonoid family [32,33], and their biosynthesis is closely associated with flavonoid biosynthesis pathways. Namely, flavonoid biosynthesis, flavone and flavonol biosynthesis pathways, and anthocyanin biosynthesis, are associated with plant coloration [34]. From the petal color phenotype, the roses used here varied from white, pink, and red to dark red. The shades of petal colors, from white to dark, may represent the number of anthocyanins, from low to high. The petals of Old Rose with the red color were lighter than in Crimson Glory and deeper than in Damascena and Iceberg, indicating that the content of anthocyanins in Old Rose is less than in Crimson Glory and more than in Damascena and Iceberg. The heat map of anthocyanins verified this inference; color modules representing high accumulation were stacked more in varieties with deeper flower colors (Fig. S9). Furthermore, the metabolic pathway analysis results also demonstrated this inference. That is, the three pathways associated with coloration were significantly enriched in the deep-colored varieties compared with the light-colored ones (Fig. 5).

Four classes of anthocyanins (cyanidin-, delphinidin-, peonidin-, and pelargonidin-derived anthocyanins) were present in these petals. It has been reported that pelargonidin-, cyanidin-, and delphinidin-based anthocyanins are involved in brick red-scarlet, red-magenta, and blue-violet colors, respectively [35]. Furthermore, cyanidin-based anthocyanin was the predominant anthocyanin in red-colored rose varieties [36,37]. This was confirmed by the significant accumulation of cyanidin 3-glucoside and cyanidin 3-rutinoside in Old Rose (Fig. S9). In addition, paeoniflorin 3-glucoside was also accumulated in this plant. The accumulation of rich anthocyanins indicates the potential value of Old Rose as a source of natural pigments in the food industry. Although delphinidins contribute blue-violet colors in some plants [33,35,38–40], delphinidins (delphinidin, delphinidin 3-glucoside, and delphinidin 3-rutinoside) were detected in pink and red petals and did not make the petals blue. The reason for this may be that the petal color is affected by diverse factors such as the pH value in a cell, metal ion content, anthocyanin content, and the proportion of different anthocyanins. It can be speculated that improving the delphinidin content, changing the cellular pH value, or supporting suitable metal ions may

change the petal color to blue or purple.

It is well known that the components of floral scent are terpenoids, benzenes/phenylpropanes, fatty acid derivatives, and others [21], and their biosynthesis was associated with the formation of floral scent in plants. Based on the floral scent phenotype, the roses used in this study were fragrant or scentless. The same phytoconstituents present in aroma roses (Old Rose, Crimson Glory, and Damascena) are likely to be related to floral fragrance. Depending on the precursor substances of floral scent composition, their biosynthetic origins can be divided into fatty acids, terpenoids, and amino acid pathways [41]. In this study, the most noticeably enriched pathways closely linked to floral scent formation were monoterpenoid biosynthesis and phenylalanine metabolism (Figs. 6 and 7).

Similar to the oil-bearing rose, the Old Rose also contains rich terpenoids, including geraniol, linalool, perillyl alcohol, geranyl diphosphate, and α-terpinene, indicating that this variety also has potential value for essential oil extraction. Furthermore, 2-phenylethanol, an important component of rose oil, was also rich in Old Rose. 2-The 2-phenylethanol accounts for more than 10 % of the total quality components of traditional Chinese rose essential oil [42,43]. This is an important reference standard for evaluating the quality of rose essential oils. Two pathways have been reported for the synthesis of 2-phenylethanol: the first converts L-phenylalanine into phenylpyruvate and then into 2-phenylethanol [44], and the second converts L-phenylalanine into phenylacetaldehyde and then into 2-phenylethanol [45–47]. Phenylpyruvate or phenylacetaldehyde were not detected in our metabolic profiles. Therefore, we speculated that there is another unknown route for the synthesis of 2-phenylethanol. The relative phenylacetic acid content was much higher in aroma roses than in non-aroma roses. Therefore, we speculate that phenylacetic acid is stored as a synthetic substrate for 2-phenylethanol in cells and converted to 2-phenylethanol under specific factors, timing, and associated conditions for emitting to the environment. This is probably the reason for the maintenance of the aromatic flavor of the rose after blooming.

5. Conclusion

The edible value of the Chongqing Old Rose is unquestionable due to its prolonged history of consumption; however, further evidence is required to establish its other potential benefits fully. The presence of anthocyanins, including cyanidin 3-glucoside, cyanidin 3-rutinoside, and peonidin 3-glucoside, in Old Rose may contribute to its red flower color. Additionally, the plant is rich in 2-phenylethanol and terpenoids, which impart a pleasant aroma and serve as the natural basis for extracting essential oils. Moreover, the presence of various active phytoconstituents with antioxidant properties in this plant suggests its potential for pharmaceutical application. Consequently, the abundant presence of beneficial natural compounds in this plant underscores its significance. It holds promise as a valuable resource for extracting essential oils and enhancing the quality of functional foods and plant-derived medications.

CRediT authorship contribution statement

Chan Xu: Writing – original draft, Validation, Methodology, Funding acquisition, Conceptualization. **Yuan Chen:** Validation, Resources, Methodology. **Zongli Hu:** Validation, Data curation. **Qiaoli Xie:** Validation, Resources, Conceptualization. **Hang Guo:** Investigation, Data curation. **Shibing Tian:** Validation, Supervision, Project administration, Conceptualization. **Guoping Chen:** Validation, Supervision, Project administration, Conceptualization.

Data availability

Data will be made available through the corresponding author (CX) upon reasonable request.

Ethics statement

The authors declare that they have followed all the rules of ethical conduct regarding originality, data processing and analysis, duplicate publication, and biological material.

Declaration of competing interest

The authors declare no known competing financial interests or personal relationships that could have appeared to influence the work reported in this paper.

Acknowledgments

We would like to acknowledge the funding support of Basic Scientific Research Projects of 2023 Chongqing Financial Special Fund (cqaas2023sjczqn008), the funding support of the Chongqing Postdoctoral Science Foundation (cstc2021jcyj-bshX0066), the funding support of the Project of Chongqing Technology Innovation and Application (CSTB2024TIAD-LUX0004), and grant support from Chongqing Human Resources and Social Security Bureau (Projects Foundation of Abroad-Studying and Returning Personnel).

Appendix A. Supplementary data

Supplementary data to this article can be found online at https://doi.org/10.1016/j.heliyon.2024.e41505.

References

[1] B. Hollingsworth, Flower Chronicles, vol. 302, University of Chicago Press, Chicago, 1988.
[2] I. Demirbolat, et al., Effects of orally consumed Rosa damascena Mill. Hydrosol on hematology, clinical chemistry, lens enzymatic activity, and lens pathology in streptozotocin-induced diabetic rats, Molecules 24 (22) (2019) 4069.
[3] W. Cui, et al., Complex and reticulate origin of edible roses (Rosa, Rosaceae) in China, Horticulture Research 9 (2022).
[4] A.S. Hegde, et al., Edible rose flowers: a doorway to gastronomic and nutraceutical research, Food Res. Int. 162 (2022) 111977.
[5] W. Zhang, et al., Research progress of edible rose, Chinese Wild Plant Resources 35 (2016) 24–30.
[6] P. Kumari, B. Bhargava, Phytochemicals from edible flowers: opening a new arena for healthy lifestyle, J. Funct.Foods 78 (2021) 104375.
[7] L. Qiu, et al., Investigation of 3D printing of apple and edible rose blends as a dysphagia food, Food Hydrocolloids 135 (2023) 108184.
[8] A.M.P. dos Santos, et al., Evaluation of minerals, toxic elements and bioactive compounds in rose petals (Rosa spp.) using chemometric tools and artificial neural networks, Microchem. J. 138 (2018) 98–108.
[9] A. Devecchi, et al., Compositional characteristics and antioxidant activity of edible rose flowers and their effect on phenolic urinary excretion, Pol. J. Food Nutr. Sci. 71 (4) (2021) 383–392.
[10] H. Friedman, et al., Characterization of yield, sensitivity to Botrytis cinerea and antioxidant content of several rose species suitable for edible flowers, Sci. Hortic. 123 (3) (2010) 395–401.
[11] J. Zheng, et al., Total phenolics and antioxidants profiles of commonly consumed edible flowers in China, Int. J. Food Prop. 21 (1) (2018) 1524–1540.
[12] N. Kumar, et al., Antioxidant activity and ultra-performance LC-electrospray ionization-quadrupole time-of-flight mass spectrometry for phenolics-based fingerprinting of Rose species: Rosa damascena, Rosa bourboniana and Rosa brunonii, Food Chem. Toxicol. 47 (2) (2009) 361–367.
[13] M.-C. Martínez, et al., Narcea—an unknown, ancient cultivated rose variety from northern Spain, Horticulture research 7 (2020).
[14] Altıntaş, A., Rose, rose water: historical, therapeutic and cultural perspectives. *Pharmacy and the History of Medicine Series*. 2010: Maestro Publishing, Istanbul, Turkey.
[15] M.H. Boskabady, et al., Pharmacological effects of Rosa damascena, Iranian journal of basic medical sciences 14 (4) (2011) 295.
[16] A. Gholamhoseinian, H. Fallah, Inhibitory effect of methanol extract of Rosa damascena Mill. flowers on α-glucosidase activity and postprandial hyperglycemia in normal and diabetic rats, Phytomedicine 16 (10) (2009) 935–941.
[17] P. Singh, et al., Potential dual role of eugenol in inhibiting advanced glycation end products in diabetes: proteomic and mechanistic insights, Sci. Rep. 6 (1) (2016) 18798.
[18] K. Rao Venkata Kurapati, et al., Natural products as anti-HIV agents and role in HIV-associated neurocognitive disorders (hand): a brief overview, Front. Microbiol. 6 (2016) 1444.
[19] N. Tran, B. Pham, L. Le, Bioactive compounds in anti-diabetic plants: from herbal medicine to modern drug discovery, Biology 9 (9) (2020) 252.
[20] E. Pichersky, J.P. Noel, N. Dudareva, Biosynthesis of plant volatiles: nature's diversity and ingenuity, Science 311 (5762) (2006) 808–811.
[21] D.R. Gang, Evolution of flavors and scents, Annu. Rev. Plant Biol. 56 (1) (2005) 301–325.
[22] N. Dudareva, E. Pichersky, J. Gershenzon, Biochemistry of plant volatiles, Plant Physiol. 135 (4) (2004) 1893–1902.
[23] A. Kessler, I.T. Baldwin, Defensive function of herbivore-induced plant volatile emissions in nature, Science 291 (5511) (2001) 2141–2144.
[24] O. Fiehn, T. Kind, Metabolite profiling in blood plasma, in: W. Weckwerth (Ed.), Metabolomics: Methods and Protocols, Humana Press, Totowa, NJ, 2007, pp. 3–17.
[25] O. Fiehn, et al., Quality control for plant metabolomics: reporting MSI-compliant studies, Plant J. 53 (4) (2008) 691–704.
[26] N. Vasilev, et al., Structured plant metabolomics for the simultaneous exploration of multiple factors, Sci. Rep. 6 (1) (2016) 37390.
[27] E. Zelena, et al., Development of a robust and repeatable UPLC− MS method for the long-term metabolomic study of human serum, Anal. Chem. 81 (4) (2009) 1357–1364.
[28] E.J. Want, et al., Global metabolic profiling of animal and human tissues via UPLC-MS, Nat. Protoc. 8 (1) (2013) 17–32.
[29] H.A. El Gizawy, et al., In vitro cytotoxic activity and phytochemical characterization (UPLC/T-TOF-MS/MS) of the watermelon (Citrullus lanatus) rind extract, Molecules 27 (8) (2022) 2480.
[30] N. Konappa, et al., GC–MS analysis of phytoconstituents from Amomum nilgiricum and molecular docking interactions of bioactive serverogenin acetate with target proteins, Sci. Rep. 10 (1) (2020) 16438.
[31] M. Talha, et al., Biological evaluation, phytochemical screening, and fabrication of Indigofera linifolia leaves extract-loaded nanoparticles, Molecules 27 (15) (2022) 4707.
[32] M.J. Melo, F. Pina, C. Andary, Anthocyanins: nature's glamorous palette. Handbook of Natural Colorants, 2009, pp. 134–150.
[33] H.E. Khoo, et al., Anthocyanidins and anthocyanins: colored pigments as food, pharmaceutical ingredients, and the potential health benefits, Food Nutr. Res. 61 (1) (2017) 1361779.
[34] Q. Lou, et al., Transcriptome sequencing and metabolite analysis reveals the role of delphinidin metabolism in flower colour in grape hyacinth, J. Exp. Bot. 65 (12) (2014) 3157–3164.
[35] Y. Tanaka, A. Ohmiya, Seeing is believing: engineering anthocyanin and carotenoid biosynthetic pathways, Curr. Opin. Biotechnol. 19 (2) (2008) 190–197.
[36] P. Kumari, et al., Characterization of anthocyanins and their antioxidant activities in Indian rose varieties (Rosa × hybrida) using HPLC, Antioxidants 11 (10) (2022) 2032.
[37] Q. Ge, X. Ma, Composition and antioxidant activity of anthocyanins isolated from Yunnan edible rose (An ning), Food Sci. Hum. Wellness 2 (2) (2013) 68–74.
[38] S.D. Castellarin, et al., Colour variation in red grapevines (Vitis vinifera L.): genomic organisation, expression of flavonoid 3'-hydroxylase, flavonoid 3', 5'-hydroxylase genes and related metabolite profiling of red cyanidin-/blue delphinidin-based anthocyanins in berry skin, BMC Genom. 7 (2006) 1–17.
[39] Y. Katsumoto, et al., Engineering of the rose flavonoid biosynthetic pathway successfully generated blue-hued flowers accumulating delphinidin, Plant Cell Physiol. 48 (11) (2007) 1589–1600.
[40] C. Hu, et al., Anthocyanin characterization and bioactivity assessment of a dark blue grained wheat (Triticum aestivum L. cv. Hedong Wumai) extract, Food Chem. 104 (3) (2007) 955–961.
[41] N. Dudareva, et al., Biosynthesis, function and metabolic engineering of plant volatile organic compounds, New Phytol. 198 (1) (2013) 16–32.
[42] L. Feng, et al., Changes of the aroma constituents and contents in the course of Rosa rugosa Thunb. flower development, Sci. Agric. Sin. 41 (12) (2008) 4341–4351.
[43] Y. Yu, Q. Wang, L. Yao, Research on the aroma constituents and contents of Rosa rugosa 'Purple branch', J. Shanghai Jiaot. Univ. 2 (2012) 80–87, 94.
[44] S. Watanabe, et al., Biogenesis of 2-phenylethanol in rose flowers: incorporation of [2H8]L-phenylalanine into 2-phenylethanol and its beta-D-glucopyranoside during the flower opening of Rosa 'Hoh-Jun' and Rosa damascena Mill, Biosci. Biotechnol. Biochem. 66 (5) (2002) 943–947.

[45] M. Sakai, et al., Production of 2-phenylethanol in roses as the dominant floral scent compound from L-phenylalanine by two key enzymes, a PLP-dependent decarboxylase and a phenylacetaldehyde reductase, Biosci. Biotechnol. Biochem. 71 (10) (2007) 2408–2419.
[46] X. Chen, et al., Functional characterization of rose phenylacetaldehyde reductase (PAR), an enzyme involved in the biosynthesis of the scent compound 2-phenylethanol, J. Plant Physiol. 168 (2) (2011) 88–95.
[47] M. Sakai, et al., Purification and characterization of β-glucosidase involved in the emission of 2-phenylethanol from rose flowers, Biosci. Biotechnol. Biochem. 72 (1) (2008) 219–221.

Dr. Chan Xu is a postdoctoral fellow at Postdoctoral Workstation of Chongqing Academy of Agricultural Sciences and Postdoctoral Research Station of College of Bioengineering, Chongqing University, Chongqing 400000, China